Construction and Building Materials 58 (2014) 171–181

Contents lists available at ScienceDirect

Construction and Building Materials

journal homepage: www.elsevier.com/locate/conbuildmat

Dedolomitization and alkali-silica reactions in low-expansive marbles from the province of Córdoba, Argentina. A microstructural and chemical study

Locati Francisco [a,*], Falcone Darío [b], Marfil Silvina [c]

[a] CICTERRA (CONICET – UNC), Av. Vélez Sarsfield 1611, X5016GCA Córdoba, Argentina
[b] UNLP – LEMIT – CIC (Province of Buenos Aires), Calle 52 y 121, B1900AYA La Plata, Argentina
[c] UNS – INGEOSUR – CIC (Province of Buenos Aires), San Juan 670, 8000 Bahía Blanca, Argentina

HIGHLIGHTS

- The potential reactivity of marbles from Córdoba (Argentina) was studied.
- Low expansions due to ASR rather than to non-expansive dedolomitization were recorded.
- Relict strained quartz and possibly fine-grained phlogopite acted as silica sources.
- The extent of dedolomitization was controlled by the content of dolomite.
- Dedolomitization in marbles and sedimentary carbonates seems to have acted similarly.

ARTICLE INFO

Article history:
Received 31 December 2013
Received in revised form 13 February 2014
Accepted 14 February 2014
Available online 7 March 2014

Keywords:
Marble
Alkali-carbonate reaction
Dedolomitization
Mg–Si–Al phase
Carbonate halo
Alkali-silica reaction
ASR gel

ABSTRACT

Marbles from the province of Córdoba (Argentina) have been used as aggregates in concrete; however, there is little information about their potential reactivity and interaction with the cement paste. Recently, the alkali-carbonate reactivity of dolomitic to calcitic marbles from this province was determined by standardized methods (ASTM C1293, ASTM C586, CSA A23.2-26A) and a modification of the Chinese Accelerated Mortar Bar Method (M-CAMBT) using a single aggregate size fraction (2.5–5.0 mm). Although all samples behaved as non-reactive some expansion was recorded, especially in the M-CAMBT method. In this work microstructural and chemical studies were carried out by stereomicroscopy, polarizing microscopy, X-ray diffraction (XRD), scanning electron microscopy (SEM) and electron probe microanalysis (EPMA) on mortar bars tested by the M-CAMBT method. Dedolomitization was detected in all dolomitic and calc-dolomitic marbles being more accentuated in the samples with more dolomite. This process is characterized by the development of different zones in the cement–aggregate interface that differ in texture and chemical composition and are similar to the zones described by other authors in dolomitic limestones typically associated with the so-called alkali–carbonate reaction. Therefore, the presence and distribution of dedolomitization appears not to be related to the texture of the aggregates but to the amount of dolomite in the rock. The low expansions recorded were associated with relict strained quartz and possibly with fine-grained phlogopite in the matrix of the rocks, which have acted as silica sources for the development of secondary silicates of variable composition (±Ca ± Na ± K ± Mg ± Al) and microfissures as a result of the alkali–silica reaction rather than the non-expansive dedolomitization process.

1. Introduction

The reactivity of carbonatic rocks in concrete has been extensively studied since 1957 when this process was first described in Canada by Swenson [1]. Thereafter, many cases of structures affected by the so-called alkali-carbonate reaction (ACR) were reported in other countries (e.g. the United States [2–5], China [6,7], Austria [8]). Katayama [9–12] restudied some Austrian and

* Corresponding author. Tel.: +54 351 5353800x30234; fax: +54 351 4344980x103.
E-mail addresses: flocati@efn.uncor.edu (F. Locati), durabilidad@lemit.gov.ar (D. Falcone), smarfil@uns.edu.ar (S. Marfil).

http://dx.doi.org/10.1016/j.conbuildmat.2014.02.019
0950-0618/

Canadian carbonatic aggregates and although dedolomitization was observed, the expansive behaviour was attributed to the reactivity of cryptocrystalline quartz present in the microstructure of those rocks, which induced alkali-silica reactions (ASRs). Similar considerations have been done in recent work on field and laboratory specimens where Canadian and Chinese aggregates were restudied [13–16].

The mechanisms that lead to concrete deterioration due to the so-called ACR are, therefore, a matter of current debate (e.g. [17] and references cited therein); however, recent studies point out that two main processes can occur separately or simultaneously depending on the mineral composition of the aggregates involved in the process: (a) dedolomitization of dolomite crystals in carbonatic aggregates and (b) ASR caused by silica minerals in the carbonatic aggregates, the first one being non-expansive and the second one expansive and the cause of concrete deterioration (e.g. [9–12,18,19]).

In 1961, Hadley [2] proposed the dedolomitization model to explain the reaction process between carbonatic aggregates and the alkalis present in the concrete pore solution, the so-called alkali-carbonate reaction. Currently, the basis of this model is widely accepted worldwide and can be described as follows.

In alkaline conditions, the dolomite present in dolomitic limestones interacts with the alkali hydroxides from the concrete pore solution causing a fine intergrowth of calcite and brucite. This process releases CO_3^{2-} from sodium carbonate, which migrates to the cement paste dissolving the portlandite phase and releasing Ca^{2+} ions that will react to form a carbonate halo around the aggregate and will keep the solution alkalinity high due to the regeneration of the alkali hydroxide [2].

In Argentina, this subject has been investigated since 1991, but so far no structures in service affected by the so-called ACR have been reported. Laboratory tests have been conducted on some carbonatic aggregates such as dolomites from Olavarría (province of Buenos Aires), dolomites from Valcheta (province of Río Negro) and dolomitic marbles from Alta Gracia (province of Córdoba) (e.g. [20–23]) in order to evaluate their potential reactivity. According to the authors, the three aggregates showed evidence of dedolomitization, but only the dolomite from Valcheta was classified as potentially reactive owing to its expansive behaviour [24]. In the latter work, the authors concluded that the dolomite aggregate from Valcheta reacts deleteriously with concrete alkalis following a mechanism similar to that of ACR. Furthermore, they claimed that it was not possible to deny that ASR could take a part in the expansive reaction, considering the potentially reactive components of the insoluble residue of the rock (in this rock the insoluble residue varies between 10% and 20% and it is composed of quartz, feldspar, fragments of rhyolitic volcanic rocks, illite, smectite and sepiolite).

In the province of Córdoba (Argentina) metamorphic carbonatic rocks (dolomitic to calcitic marbles) are incorporated in the concrete as coarse aggregates, but generally as part of a mixture of rocks of variable composition, gneisses being the main lithology exploited. Locati et al. [25] studied a highway in Córdoba that shows evidence of deterioration due to the ASR. The aggregates utilized in the structure were biotitic gneisses, migmatites, marbles, amphibolites, and granitic to tonalitic rocks, affected by deformation processes of variable intensity. The authors concluded that metamorphic quartz-bearing aggregates that present internal deformation microstructures played an important role in the deterioration producing slow/late expansions. However, no deterioration linked with marbles was observed.

Although the characteristics of these rocks differ from those of the sedimentary carbonatic rocks associated with the so-called ACR (argillaceous dolomitic limestones with dolomite rhombs scattered in the fine-grained matrix), in other parts of the world there are some records about the reactivity of carbonatic rocks that differ from the traditional ones ([26] and references cited therein). According to Katayama [9] "...it is recommended that concrete petrographers make a careful examination of the carbonate aggregates without prejudice, not only focusing on the well-known type of reactive argillaceous dolomitic limestone, but also covering the whole range of the carbonate rocks found in the concrete...".

Considering that there are laboratory records about dedolomitization processes in marbles from Alta Gracia in the province of Córdoba (Argentina) [20] and besides, that these aggregates (and other marbles from this province) can contain accessory minerals in variable proportions (such as strained quartz), the reactivity of four marbles from Córdoba has recently been assessed [27] by standardized methods such as ASTM C1293 [28], ASTM C586 [29] and CSA A23.2-26A [30]. The samples were also tested by a modification of the Chinese accelerated mortar bar method (M-CAMBT) after Lu et al. [31] using a single aggregate size fraction (2.5–5.0 mm), which is a modified version of the method to evaluate ASR proposed by Xu et al. [32]. According to the authors [31], this is a quick and reliable test to evaluate both potential alkali-silica and alkali-carbonate reactivity of concrete aggregates.

All samples studied behaved as non-reactive in all tests, although some expansion was recorded (always below the acceptance limit), especially in the M-CAMBT method. In addition, preliminary observations under polarizing microscopy in mortar bars after being tested showed the development of both empty and partially filled microfissures in the cement paste and brownish rims around some dolomite-bearing aggregates.

In this work microstructural and chemical studies by stereomicroscopy, polarizing microscopy, XRD, SEM and EPMA were carried out on mortar samples after being tested by the M-CAMBT method in order to determine the presence of dedolomitization and ASR processes in the marbles from the province of Córdoba (Argentina) and to evaluate their influence on the low expansions recorded.

2. Materials and methods

2.1. Materials

Mortar bars were studied after being tested by the M-CAMBT method [31]. This test consists in making three short-fat bars (40 × 40 × 160 mm), at fixed cement–aggregate ratio of 1:1 and water-cement ratio of 0.33. The moulds are covered with a plastic sheet and stored in a fog room at 23 °C for 24 ± 2 h. The bars are then demoulded and immersed in water in sealed plastic containers and placed in an oven at 80 °C for 24 ± 2 h. Then the initial length measurement is taken and the bars are transferred to containers filled with 1 N NaOH solution at 80 °C, which are returned to the oven maintained at 80 °C. The lengths of the bars are periodically measured. An acceptance limit of 0.093% at 14 days is taken to evaluate alkali-silica reactive aggregates and 0.1% at 28 days to evaluate alkali-carbonate reactive aggregates.

A normal portland cement with compressive strength ⩾40 MPa at 28 days, denominated CPN40 [33], similar to ASTM Type I [34], of low-alkali content was used (0.35% Na_2O_{eq}). The Na_2O_{eq} was adjusted to 1.5% by adding KOH to the mixing water. The aggregate samples were crushed to obtain a 4.75–2.36 mm single size fraction determined by standardized sieves in accordance with Argentine standards [35], the 2.36–4.75 mm range being similar to the 2.5–5 mm range proposed by Lu et al. [31]. The results of the M-CAMBT method can be seen in Fig. 1.

The aggregates tested come from the province of Córdoba (Argentina). Three of the samples are monolithologic (DM, MM and CDM) and one is polylithologic (PL). Mineralogy was determined by petrography and XRD on natural samples and on the insoluble residue. Mineral abbreviations after Whitney and Evans [36] were adopted.

DM (Figs. 2a and 3a): Dolomitic marble (Dol >> Cal ± Srp ± Tlc ± Chl ± Phl ± Di) with granoblastic texture (grains ⩽8 mm) and evidence of recrystallization in grain boundaries (recrystallized grains ⩽0.1 mm). The rock contains ~5% phlogopite, talc and serpentine.

MM (Figs. 2b and 3d): Mylonitic marble (Cal ± Di ± Qz ± Tr ± Pl ± Ttn, without Dol) with porphyroclastic texture due to shear deformation. The matrix is composed of small oriented and partially recrystallized calcite grains (~20 μm). Porphyroclasts (~10% of the rock) are composed of calcite (individual or multiple grains), diopside ± tremolite aggregates, gneissic aggregates, and titanite, quartz, plagioclase individual grains (⩽8 mm). Quartz (<5%) shows undulatory extinction and scarce small subgrains (~50 μm).

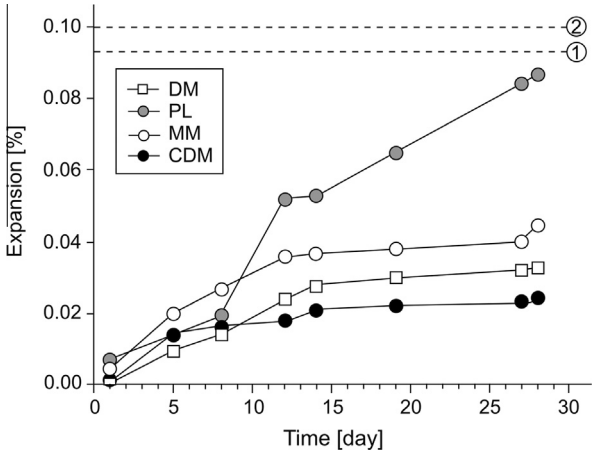

Fig. 1. Expansion of mortar bars after the M-CAMBT method [31]. Dashed lines indicate acceptance limits for ASR (1) at 14 days (0.093%) and ACR (2) at 28 days (0.01%).

CDM (Figs. 2c and 3b): Calc-dolomitic marble (Dol > Cal ± Phl ± Srp ± Qz ± Spl ± Ol ± Opq) with granoblastic texture (grains ⩽3 mm). The rock is composed of ~5% phlogopite and ~15% serpentine. Quartz is scarce (<1%) and shows no evidence of deformation.

PL (Figs. 2d–f and 3c): This sample was extracted from a stockpile of aggregates for construction in a quarry and is composed of aggregates of variable composition (polylithologic sample). Calc-dolomitic marble (Cal > Dol ± Phl ± Di ± Srp ± Tr ± Ol) prevails (~50%, Fig. 3c). It has granoblastic texture (Fig. 2d) with grains ~1 mm, but variable, and ~40% accessory minerals. The other ~50% of the mixture is composed of tonalitic intrusive rocks, biotitic paragneisses containing garnet and orthogneisses rich in clinopyroxene and amphibole in variable proportions (paragneisses being dominant, Fig. 2e). Both gneisses and tonalitic intrusives contain quartz (grains ⩽1 mm) with marked undulatory extinction and showing the development of deformation bands ~40 μm wide (Fig. 2f).

2.2. Methods

2.2.1. Characterization of the aggregates tested

Petrographic descriptions on thin sections (~20 μm thick) of the aggregates utilized in the mortar bars (Section 2.1 and Fig. 2) were performed using a Leica DM EP polarizing microscope (magnification of 500×) in plane-polarized light (PPL) and cross-polarized light (XPL). The percentage of insoluble residue (Fig. 3) was determined by ASTM D3042 standard [37]. Mineralogical characterization (Section 2.1 and Fig. 3) was complemented by XRD studies on natural samples and on the insoluble residue fraction with a Rigaku D-Max III-C diffractometer, working at 35 kV and 15 mA, using Cu $K\alpha_{1,2}$ radiation (λ = 1.541840 Å) filtered with a graphite monochromator in the diffracted-beam, between 3 and 60° 2θ. Polished plates (abrasive size up to 9 μm) of marble samples were stained by Alizarine Red S (0.3 g of alizarine in 100 ml of 1.5% HCl solution) adapting the procedure after Hutchison [38] for thin sections. Images of stained plates were obtained and transformed into binary images (Fig. 3). Then, calcite percentage was determined by ImageJ software [39] on the 2D section. Additionally, quantification of mass fractions of the mineral phases identified by XRD on natural calcareous samples was done by X'Pert High-

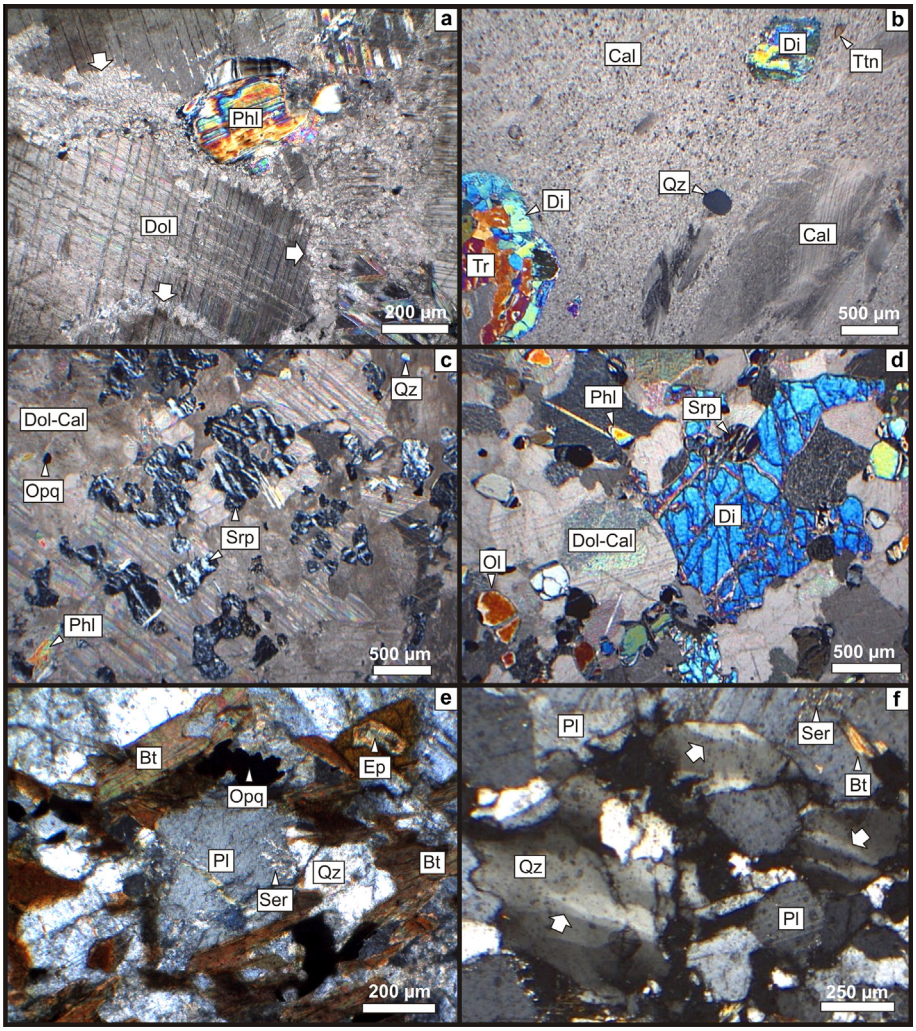

Fig. 2. Photomicrographs (cross-polarized light). (a) Sample DM: dolomitic marble (Dol >> Cal) with evidence of recrystallization in grain boundaries (white arrows). (b) Sample MM: mylonitized marble (without Dol) with a calcitic matrix. (c) Sample CDM: serpentinic marble (Dol>Cal). (d) Calc-dolomitic marble (Cal>Dol) from sample PL. (e) Biotitic paragneiss from sample PL. (f) Tonalitic intrusive from sample PL showing quartz grains with marked undulatory extinction and deformation bands (white arrows).

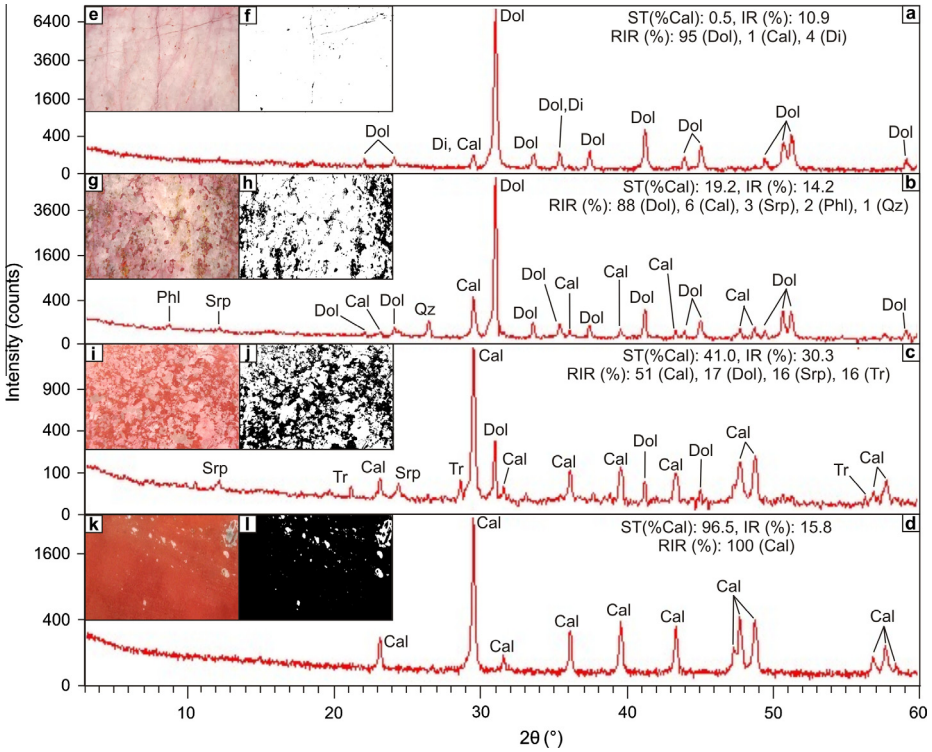

Fig. 3. Diffraction patterns of natural marble samples DM (a), CDM (b), PL (c) and MM (d). Polished rock plates stained by Alizarine Red S and binary image of the stained rock plates DM (e,f), CDM (g,h), PL (i,j) and MM (k,l). ST(%Cal): Calcite determined by staining technique, IR (%): Insoluble residue, RIR (%): Semi-quantitative percentages estimated by the Reference Intensity Ratio. (For interpretation of the references to colour in this figure legend, the reader is referred to the web version of this article.)

Score software (PANalytical) using the scale factor and Reference Intensity Ratio (RIR) values from database ICDD (International Centre for Diffraction Data). The analysis of the program is semi-quantitative and uses the RIR method proposed by Chung [40].

2.2.2. Studies performed on tested mortar bars

2.2.2.1. Stereomicroscopy and polarizing microscopy. Tested bars were studied by a stereomicroscope (magnification of 40×) in order to detect cracks, changes in coloration in the cement paste or in the cement–aggregate interfaces and the formation of secondary products. For this purpose, broken surfaces of the mortar bars and polished mortar slabs (4.5 × 2.5 × 0.5 mm, abrasive size up to 9 μm) were studied. Secondary products were separated, if possible, from the mortar bars with a stainless-steel needle for their study. Petrographic analyses on thin sections were also performed focusing on cement–aggregate interfaces and microfissures using the aforementioned microscope (Section 2.2.1).

2.2.2.2. XRD. In order to identify the crystalline phases present in the rim zone of the calcareous aggregates after the test, the material was carefully scraped off a thin section with a stainless-steel needle under the polarizing microscope and was placed directly on a single-crystal silicon sample holder. The crystalline phases were identified with a PANalytical X'Pert PRO diffractometer, working at 40 kV and 40 mA, using Cu $K\alpha_{1,2}$ radiation (λ = 1.541840 Å) filtered with a graphite monochromator in the diffracted beam. Due to the small amount of material collected, a relatively slow scanning from 5° to 55° 2θ with increments of 0.02° 2θ and a counting time of 20 s per step was performed.

2.2.2.3. SEM. The reaction products separated under the stereomicroscope were analysed with a LEO 1450VP microscope equipped with an energy dispersive X-ray spectrometer (EDS) for semi-quantitative analyses, working at 15 kV. Additionally, complementary textural and chemical studies on carbon-coated polished thin sections (abrasive size up to 1 μm) were performed using a Carl Zeiss FE (Field Emission)-SEM Σigma microscope of high resolution equipped with an EDS. Compositional maps (Mg, Ca, Si, Al, Na and K) were obtained working at 8 kV. The peak intensity of carbon (at ~0.3–0.4 keV) in EDS spectra is very variable and it was not considered in the analysis because it corresponds to a sum of energies from carbon in the sample, carbon from the coating, calcium L lines, etc. Secondary electron (SE) images and backscattered electron (BSE) images were obtained.

2.2.2.4. EPMA. Compositional maps (Mg, Ca, Si, Al, Na and K) of the cement–aggregate interface after the test were obtained using a JEOL JXA 8230 microscope equipped with two wavelength dispersive spectrometers (WDS) and one integrated EDS. Analytical conditions used for mapping were 15 kV, 20 nA, beam diameter = 1 μm and counting time per pixel = 50 ms. A carbon-coated polished thin section (abrasive size up to 1 μm) was utilized. BSE images were obtained.

3. Results

3.1. Macroscopic observations

At macroscopic level, mortar bars are in good condition. Some carbonatic aggregates (dolomitic to calc-dolomitic marbles) show the development of a discontinuous white rim zone (~320 μm wide) in contact with the cement paste that is also found on both sides of original internal microcracks in the carbonatic aggregates. The cement paste becomes clearer (an area ~50 μm wide) in contact with the white zones but not where this discontinuous rim is absent. Some microfissures associated with carbonatic and non-carbonatic aggregates are detected in the paste or in the cement–aggregate interface (Fig. 4a–c). In localized areas, reaction products partially filling cavities were detected. Massive transparent and opaque white materials were separated for their study. The transparent material is flexible and does not break when it is pressed with a steel needle, while the white material is rigid and breaks easily.

3.2. Petrographic observations

At microscopic level, the cement paste is in good condition, although some microfissures (5–30 μm wide) in the paste or in the cement–aggregate interface can be seen (Fig. 5), its abundance being in relation to the expansion measured in the M-CAMBT

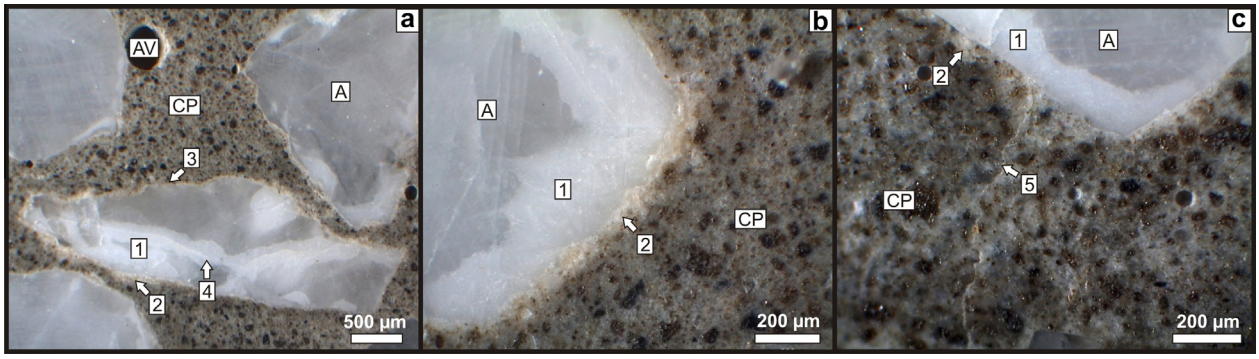

Fig. 4. Macroscopic observations. (a) Sample DM showing discontinuous white rims and internal microcracks with white material on both sides. (b) Detail of the white rim. (c) Microfissure in the cement paste associated with the dolomitic aggregate. A: aggregate, CP: cement paste, AV: air void, 1: white reaction rim, 2: carbonated cement paste, 3: non-carbonated cement paste, 4: white reaction material on both sides of an internal microcrack, 5: microfissure in the cement paste.

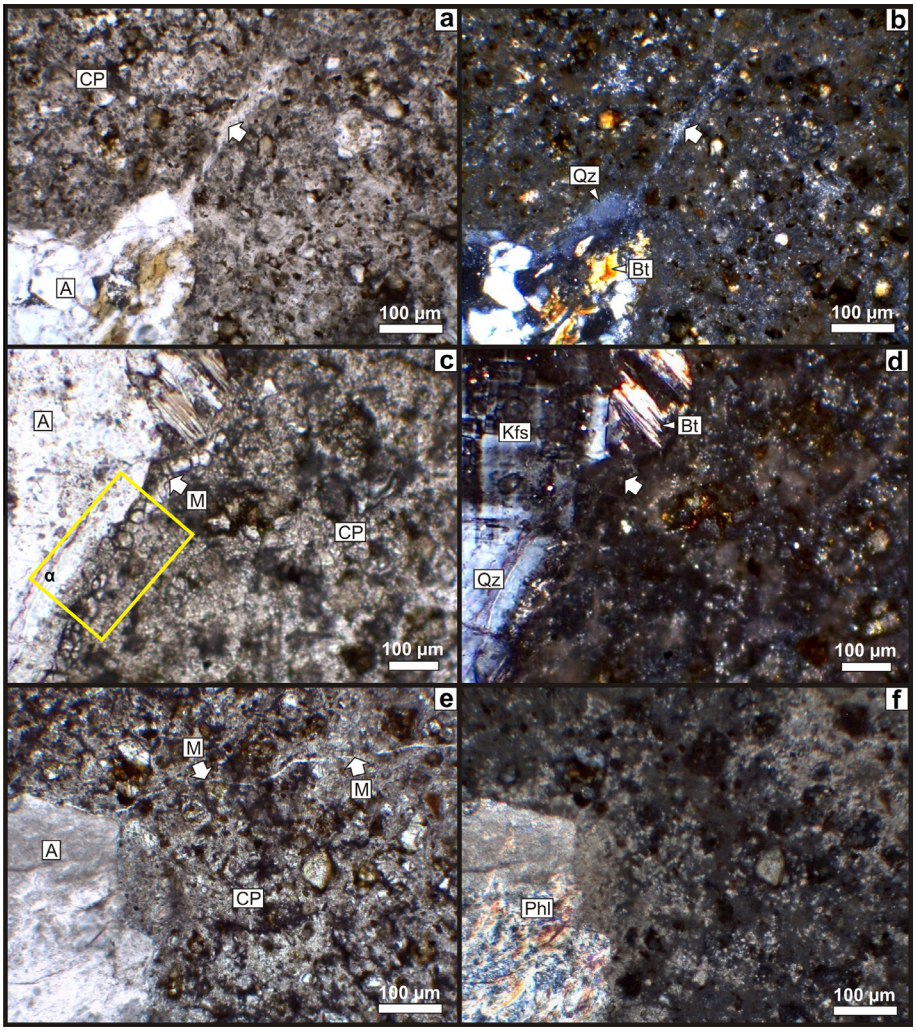

Fig. 5. Photomicrographs (a, c, e – PPL, b, d, f – XPL). (a and b) Material of low interference colour (white arrow) extruded from a gneissic aggregate (sample PL). (c and d) Microfissure (~40 µm wide) in the cement–aggregate interface (white arrow) filled with a cracked material of low interference colour (sample PL). Square α: sector studied by SEM-EDS in Fig. 7c–e. (e and f) Microfissure in the cement paste associated with a dolomitic aggregate containing phlogopite (sample DM). A: aggregate, CP: cement paste, M: microfissure.

(PL > MM > DM > CDM). Some of them are filled with "gel" of low interference colour (Fig. 5b and d) and are mostly linked to gneisses or tonalitic intrusives containing strained quartz in the bars made with sample PL (Fig. 5a–d), to porphyroblasts with quartz in the bars made with sample MM or to marbles containing fine-grained phlogopite (⩽100 µm) in the bars made with samples DM and CDM (Fig. 5e and f).

Some carbonatic aggregates (dolomitic to calc-dolomitic marbles) showed the development of discontinuous dark brownish rims recognizable in PPL (Fig. 6a, d and e). These brownish rims

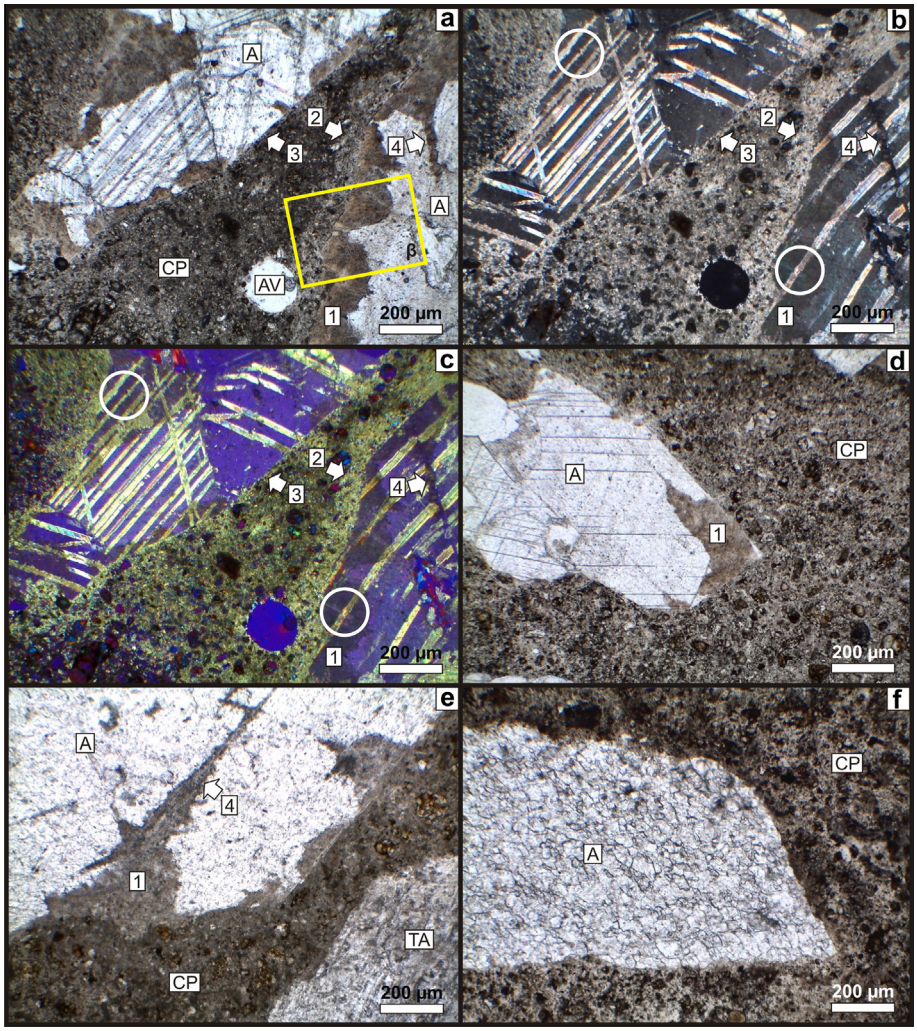

Fig. 6. Photomicrographs (a, d–f – PPL, b – XPL, c – XPL and gypsum plate added). (a–c) Brownish material in DM sample boundaries with optical continuity with the original crystals of dolomite (white circles). Square β: sector studied by EPMA in Fig. 8. (d) Brownish material in sample CDM. (e) Brownish material in dolomitic aggregate (sample PL). (f) Mylonitic marble (MM) showing no development of a brownish rim. A: carbonatic aggregate, TA: tonalitic aggregate, CP: cement paste, AV: air void, 1: dark brownish rim, 2: carbonated cement paste, 3: non-carbonated cement paste, 4: dark brownish material on both sides of an internal microcrack. (For interpretation of the references to colour in this figure legend, the reader is referred to the web version of this article.)

are poorly identified in XPL (Fig. 6b), unless a gypsum plate is added (Fig. 6e). These zones (⩽300 μm wide) show optical continuity with the original crystals of dolomite (white circles, Fig. 6b and c). Their abundance (DM > CDM > PL) is in relation to the proportion of dolomite present in the aggregates (Fig. 3). Bars made with sample MM show no evidence of this process (Fig. 6f). The cement paste associated with brownish zones is highly carbonated (areas with high interference colour, ⩽90 μm wide), whereas the cement paste associated with non-reacted areas is non-carbonated (cf. 2 and 3 in Fig. 6b and c). Sometimes this darkening of the aggregate is also found on both sides of the original internal microcracks of the aggregates (Fig. 6b and e).

3.3. XRD, SEM-EDS and EPMA

The massive transparent and opaque white materials separated from the mortar bars made with sample DM were studied by SEM-EDS. They correspond to silicates that have a composition typical of ASR gel. At higher magnification, the massive transparent material shows irregular morphology with undefined habit (Fig. 7a) and according to the EDS spectrum, it is a sodium silicate with low potassium content (uncarbonated gel). The massive opaque white material consists of a set of irregular agglutinated spheres that have a sponge-like appearance (Fig. 7b). According to the EDS spectrum, it is a calcium and sodium silicate with low potassium content (carbonated gel).

ASR gel filling microfissures in the cement paste, in the cement–aggregate interface and inside the aggregates, especially in mortar bars made with samples MM and PL, were also detected. Fig. 7c shows the development of a cracked silicate in the cement–aggregate interface of a gneissic aggregate of the mortar made with sample PL (sector α in Fig. 5c). This material shows undefined morphology and variable chemical composition (different grey tones in the backscattered electron image). According to the EDS spectra, it corresponds to a silicate and/or aluminosilicate with sodium, potassium, calcium and magnesium in variable proportions. A microfissure (∼5 μm wide) filled with this silicate is also observed inside the gneissic aggregate at the top of Fig. 7c. A similar scenario was observed in the mortar bars made with sample MM.

EPMA studies on the cement–aggregate interface of a dolomite-rich aggregate in a mortar bar made with sample DM (Fig. 8a) allowed identifying different compositional zones (Fig. 8b). Zone 0 corresponds to the relict dolomitic aggregate, i.e. the interior of the aggregate that was not altered by chemical attack. A relatively

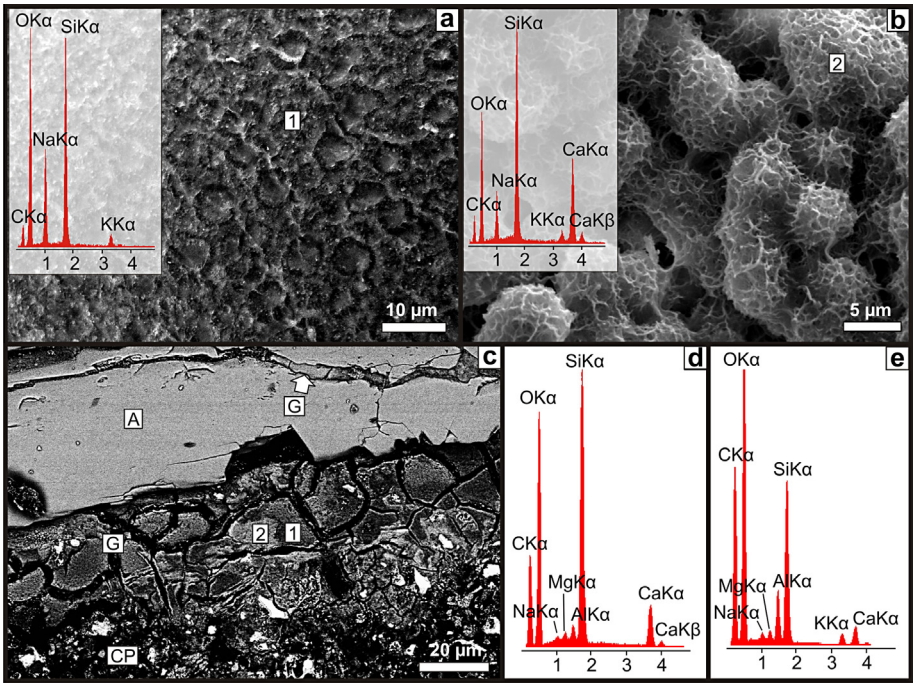

Fig. 7. SEM-EDS analyses. (a) Massive transparent material (SE image) and EDS spectrum determined in point 1. (b) Massive opaque white material (SE image) and EDS spectrum in point 2. (c) BSE image of sector α in Fig. 5c obtained by FE-SEM. (d, e) EDS spectra determined in points 1 and 2, respectively. CP: cement paste, A: aggregate, G: ASR gel.

homogeneous distribution of Ca and Mg is observed (Fig. 8c and d). Zone 1, which comprises the brownish area in the rim zone of the dolomitic aggregate, shows Ca and Mg enrichment. This enrichment is not homogeneous as zones enriched in Ca and depleted in Mg (>Ca, <Mg) and zones enriched in Mg and depleted in Ca (>Mg, <Ca) can be differentiated (Fig. 8c and d). Zone 2 (defined as the carbonated cement paste zone by petrography) is divided into three subzones. Zone 2′ is a fine layer of material (5–10 μm thick), rich in Mg, Al and with minor amounts of Si and Ca (Fig. 8c–f). Zone 2″ is an irregular band (10 to 50 μm thick) with very high Ca content (Fig. 8d). Zone 2‴ (~50 μm thick) is an irregular band enriched in Si with minor amounts of Mg, Ca, Al, Na and K (Fig. 8c–h). Na and K are more concentrated near zone 2″ and their contents decrease towards zone 3. Finally, zone 3 corresponds to the hydrated cement paste where Ca, Si and Al prevail (Fig. 8d–f).

Although these zones were identified in a mortar bar made with sample DM, the same zones were recognized in samples that showed similar cement–aggregate interfaces (samples CDM and PL).

A more detailed study of zones 1 and 2 (2′, 2″, 2‴) in the "sector γ" of Fig. 8b was performed by FE-SEM (Fig. 9a–d). At this scale, zones 2′, 2″ and 2‴ are well differentiated. Zone 2′ is a thin sector at the aggregate boundary showing regular limits towards zone 2″ and irregular limits towards zone 1 (Fig. 9a). According to the EDS spectrum (Fig. 9b), it corresponds to a material rich in Mg with minor amounts of Al and Si (Ca is variable and sometimes can be determined but in general it is under the detection limit of the EDS). Zone 2″ is a thicker sector in the cement paste, next to the aggregate boundary composed of calcium carbonate (Fig. 9c). Zone 2‴ is an irregular band and according to the EDS spectrum it corresponds to a silicate with minor (but variable) amounts of Mg, Ca, Al, Na and K (Fig. 9d).

Zone 1 at the aggregate boundary (the brownish material) shows a very particular texture of black and light grey material intergrowth resembling the graphic texture of K-feldspar and quartz in igneous rocks (e.g. [41]). This texture was previously reported as "mottled" (e.g. [9,10,18]) or "myrmekitic" (e.g. [9,19]). Because both "graphic" and "myrmekitic" textures have petrological connotations, in this case the term "mottled" is preferred. In this zone two grain sizes can be differentiated, one ranging from 10 to 5 μm and the other ⩽3 μm. In order to determine the crystalline phases present in this zone, an XRD study was performed. Due to the small amount of the material collected for the analysis, a detailed scanning (total scan time, ~14 h) was performed (see Section 2.2.2.2). Although high intensity was not achieved in the reflections observed, calcite and brucite were identified as the constituent phases (Fig. 9e). Textural relationships between both phases were studied by backscattered electron image and compositional maps of Ca and Mg were determined by FE-SEM in a dolomitic sector of a calc-dolomitic aggregate from a mortar bar made with sample PL (Fig. 9f–h). Platy crystals of brucite (white circles) intergrown with calcite (white squares) were observed. The limit between zones 1 and 0 (relict dolomite) is irregular.

4. Discussion

The ACR is still a matter of current debate. However, in some cases the lack of detailed studies could be the cause of misinterpretations and, therefore, of arriving at erroneous conclusions. For this reason, detailed studies and the combination of analytical techniques (e.g. stereomicroscopy, polarizing microscopy, XRD, SEM-EDS, EPMA) are highly recommended.

The texture of the marbles studied in this work, as well as their geological history, significantly differs from that of sedimentary carbonates studied worldwide, and although aggregates show no deleterious behaviour, some expansion was recorded. Combined studies carried out on these samples confirmed that the so-called ACR is a combination of expansive ASR and harmless dedolomitization, as was concluded by Katayama and other authors (e.g. [9–12,18,19]).

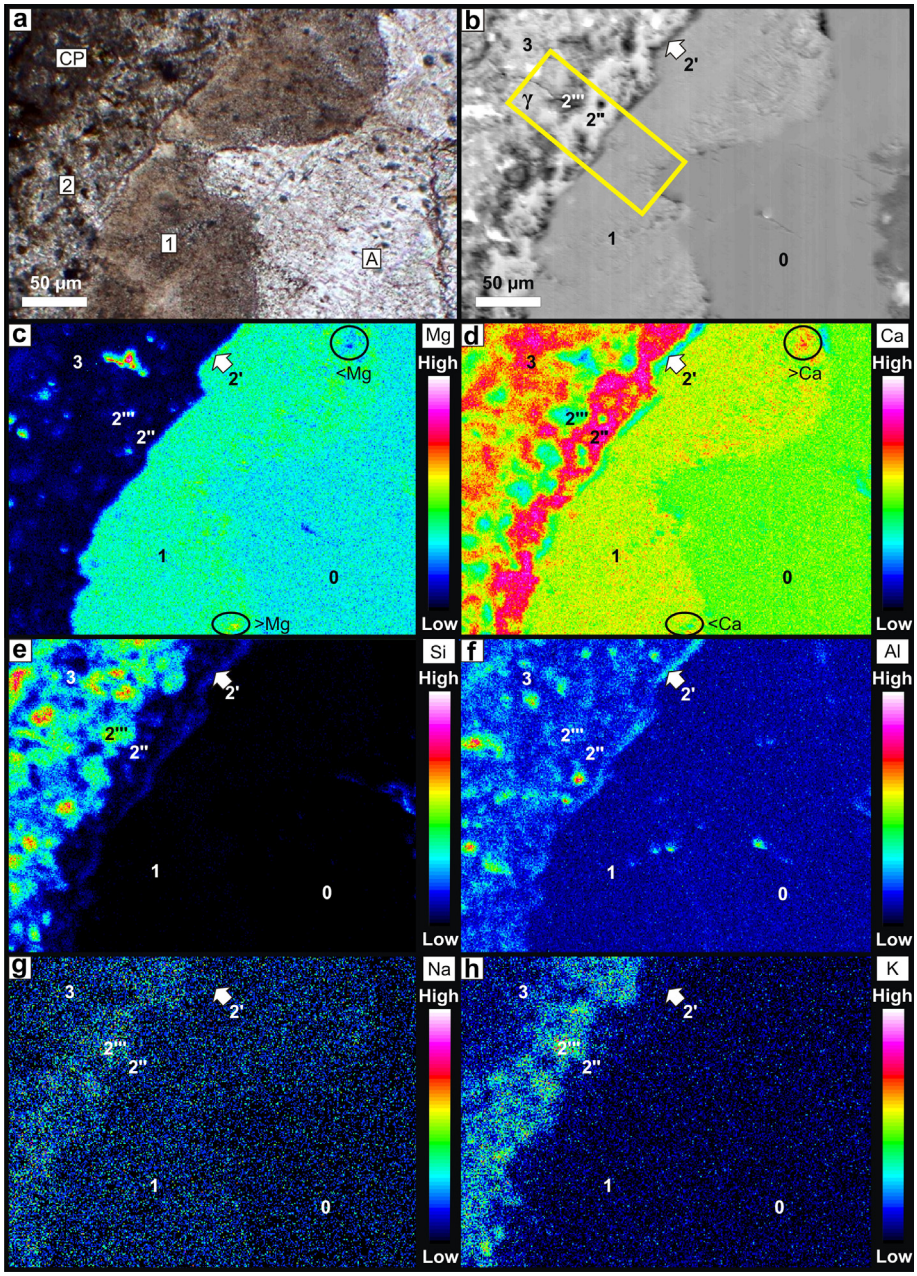

Fig. 8. (a) Photomicrograph of sector β in Fig. 6a (PPL). CP: cement paste, A: aggregate, 1: dark brownish rim, 2: carbonated cement paste. (b) Same sector obtained by EPMA (BSE image). Square γ: sector studied by FE-SEM-EDS in Fig. 9a–d. (c–h) Compositional maps of Mg (c), Ca (d), Si (e), Al (f), Na (g) and K (h) of the same sector determined by EPMA. (For interpretation of the references to colour in this figure legend, the reader is referred to the web version of this article.)

Calcite and brucite intergrowths with mottled texture (dedolomitization) were determined in the dolomite crystal boundaries that were in contact with the cement paste or on both sides of pre-existing microcracks in the carbonatic aggregates. The intergrowths replace dolomite leaving pseudomorphs of this mineral phase as proposed by Katayama [9–12], which is evidenced in this study by the optical continuity of the original host dolomite crystals that enclose small inclusions of the new calcite and brucite intergrowths (e.g. see optical continuity of dolomite twins in Fig. 6b and c).

The degree of dedolomitization was proportional to the content of dolomite determined in the rocks (DM > CDM > PL), as proposed by Katayama [9], and not related to the texture of the aggregates. The mortar bars made with sample MM showed no evidence of dedolomitization because the calcareous aggregates are calcitic in composition, ruling out the possibility of dedolomitization processes. However, the presence of strained quartz porphyroclasts would have contributed to the development of microfissures filled with neoformation products.

The expansions of the mortar bars tested were not related to the content of dolomite in the rocks but to the presence of microfissures in the cement paste and in the cement–aggregate interface (PL > MM > DM > CDM). According to microscopic observations, these microfissures were associated with gneisses or tonalitic intrusives containing strained quartz, porphyroblasts with strained quartz or marbles containing fine-grained phlogopite (⩽100 μm).

It is well known that quartz with microstructures associated with deformation processes (such as undulatory extinction, deformation bands and subgrains) as constituent of concrete aggregates can contribute to expansions due to the ASR (e.g. [42]). In addition, ASR gel with variable amounts of Na, K, Ca, Al and Mg was mainly detected in contact with those aggregates. Then, ASR was inter-

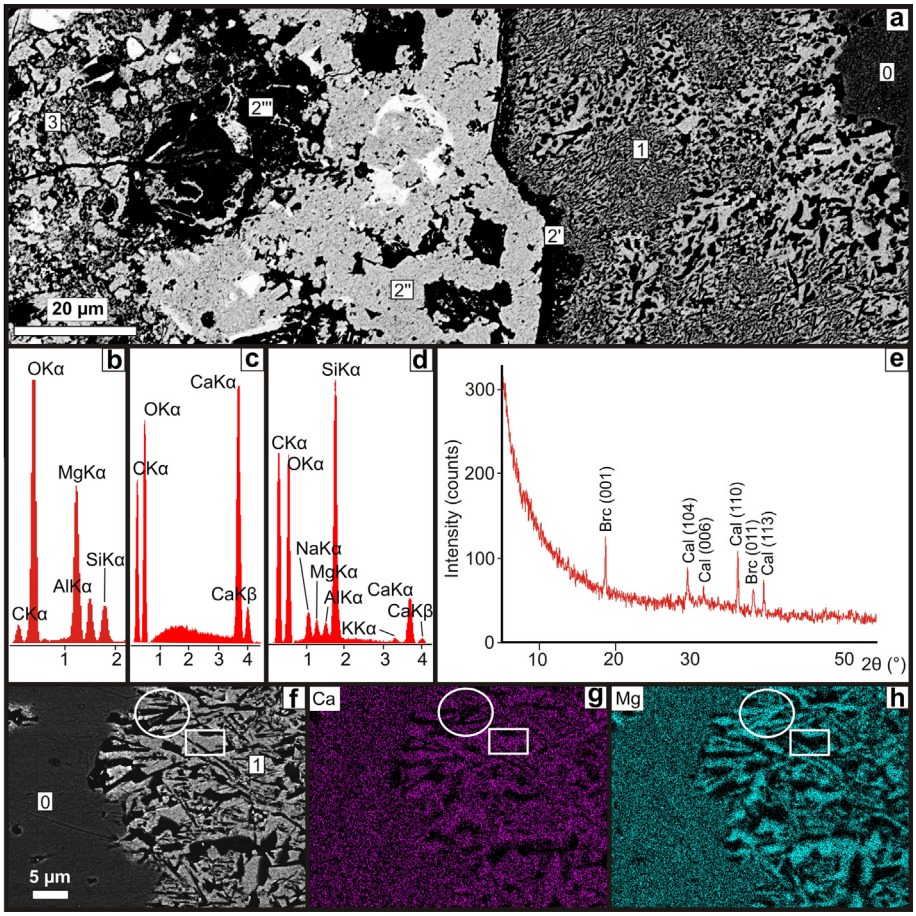

Fig. 9. (a) Sector γ in Fig. 8b obtained by FE-SEM (BSE image). (b) EDS spectrum of zone 2′. (c) EDS spectrum of zone 2″. (d) EDS spectrum of zone 2‴. (e) Diffraction pattern of the brownish material in zone 1. (f) BSE image of the brownish zone in a dolomite-rich sector of sample PL obtained by FE-SEM. (g) Compositional map of Ca. (h) Compositional map of Mg. 0: relict dolomite-rich sector. 1: brownish rim (calcite + brucite). White circle: platy crystals of brucite. White square: calcite. (For interpretation of the references to colour in this figure legend, the reader is referred to the web version of this article.)

preted as the main cause of the expansions measured on the mortar tested.

The bars made with sample DM (without quartz) showed the development of microfissures associated with aggregates with fine-grained phlogopite (⩽100 μm). In addition, although the rock has no quartz, scarce neoformation silicates with variable amounts of Na, K and Ca filling cavities were detected. It is known that phlogopite can dissolve in alkaline solution [43] releasing potassium to the concrete pore solution [44]. According to Lagerblad [45], biotite dissolves at high pH and the rate of dissolution increases with pH. This process breaks the silicate structure releasing not only potassium but aluminium and silicate complexes (and possibly other ions such as Mg and Fe) that could form part of the concrete pore solution. Therefore, phlogopite could be the source of the development of the scarce neoformation silicates identified in this sample. However, more studies are needed to confirm this interpretation.

The formation of a thin sector at the aggregate boundary next to the dedolomitized zone (zone 2′ in Figs. 8 and 9) rich in Mg, Al and Si was already recognized in other studies (e.g. [9–12,15,18,19,46]). Some authors [9,10,15] recognized a Mg-silicate gel (with minor Al, Ca, Na, K, Fe, S) next to the dedolomitized zone, attributing its formation to the interaction between brucite (product of the dedolomitization process) and an early formed ASR-gel. According to the authors, this silicate would be less expansive than the typical silicates associated with the ASR. According to Katayama [12], in aged ACR-affected concrete from near Kingston, Ontario, Mg-silicate gel tends to be more or less crystalline, having compositions of sepiolite and antigorite.The occurrence of this phase and the mechanisms involved in its formation were criticized by Xiaoming et al. [47]. However, a similar material (Mg–Si–Al phase) was recently recognized and described by Prinčič et al. [18] and Štukovnik et al. [19] proposing a chemical reaction between Si and Al ions from the cement binder and the dedolomitized aggregate as the forming mechanism. Katayama and his coworkers reported the formation of a Mg–Al phase (hydrotalcite) on the periphery of reacted dolomite crystals in concrete, where Al came from portland cement [46] and high-alumina cement [16].

In addition, Štukovnik et al. [19] evaluated the expansion process in some carbonatic aggregates from Slovenia and detected an increase in the compressive strength of dolomite aggregates compared to limestone aggregates. That gain in strength of rocks with a large amount of dolomite was already observed by Batic et al. [48] and linked with the dedolomitization products that improved mortar-rock bond in calcitic dolostone from Olavarría (Argentina). According to Štukovnik et al. [19], the explanation for this behaviour was a better interlocking between the portland cement binder and grains, due to the formation of a new Mg–Si–Al phase both in the interfacial transition zone and along pre-existing cracks in the aggregate grains and denser binder along the edges of the dedolomitized grains due to the formation of secondary calcite.

Next to zone 2′ a sector rich in calcium (zone 2″ in Figs. 8 and 9) was detected and defined as the well-known carbonate halo [9]. This supports the theory of migration of the CO_3^{2-} released during the dedolomitization reaction towards the cement paste, dissolving the portlandite phase (and possibly other calcium silicates) to produce Ca^{2+} ions. Finally, calcite is deposited at the cement–aggregate interface (of greater porosity) forming the carbonate halo.

According to Katayama [10], in the carbonation of the cement paste, the C–S–H gel may decompose to calcite and an alkali silicate that may be soluble in water and diffuse towards the pores present in the cement paste around the carbonate halo. This silicate can recombine with calcium ions to regenerate C–S–H gel through a harmless pozzolanic reaction [10,49], leaving an alkali-rich halo in the contact area, as was observed in zone 2‴ (Figs. 8 and 9).

Finally, zone 3 (Figs. 8 and 9) corresponds to the hydrated cement paste that was not affected by the dedolomitization process. In this zone, calcium hydroxides, silicates, aluminates and aluminosilicates, which are the traditional hydration products of hydrated cement, are abundant.

It is evident that more studies on the so-called ACR are needed. However, as Katayama pointed out [9–11], the term ACR should be used carefully because there is no strong evidence in this work or in the literature of deleterious expansions related to one of the main processes associated with this reaction, dedolomitization.

5. Conclusions

Marbles have been used worldwide for construction purposes; however, no detailed microstructural and chemical information about their behaviour in alkaline conditions and their interaction with the cement paste is available. This paper addresses such behaviour in dolomitic to calcitic marbles from the province of Córdoba (Argentina). From the results obtained in this work, the following major conclusions can be drawn:

- Although none of the mortar bars made with the studied aggregates exceeded the limits established by the M-CAMBT method, low expansions were detected. Detailed studies allowed correlating those expansions with microfissures and neoformation products related to the ASR rather than to dedolomitization. Therefore, ACR is a term that should be avoided or used carefully because it is a combination of the expansive alkali-silica reaction due to reactive silica minerals in the texture of the rocks and non-expansive dedolomitization (if the rock has dolomite), as Katayama clarified and re-defined [9–12].
- The relict strained quartz and possibly the fine-grained phlogopite ($\leqslant$100 μm) in the marbles have acted as silica sources for the development of neoformation silicates of variable composition (±Ca ± Na ± K ± Mg ± Al) recognized in cavities and microfissures as result of the ASR.
- In accordance with recent studies the dedolomitization process is characterized by different zones. These zones can be described as follows (from the aggregate to the cement paste):
  a. A brownish rim (under polarizing microscope) in the dolomitic aggregates consisting of a calcite and brucite intergrowth with mottled texture that replaces original dolomite crystals leaving pseudomorphs of this mineral;
  b. a thin zone (5–10 μm thick) rich in Mg, Si and Al, recognized by other authors as a Mg–Si–Al phase or a Mg-silicate gel that could contain other elements in variable proportions (e.g. Ca, Na, K, Fe, S);
  c. an irregular carbonate halo (calcite) and;
  d. an alkali-rich halo in the cement paste.

However, further chemical and microstructural detailed studies on zones *b* and *d* (zones 2′ and 2‴ in this study) are needed in order to advance in the characterization of these materials and the processes involved in their formation.

- The dedolomitization process was observed in all mortar bars tested except in those made with sample MM due to its non-dolomitic composition. In the other samples, the degree of dedolomitization was proportional to the content of dolomite determined in the rocks (DM > CDM > PL).
- The metamorphic rocks studied in this work have textures (medium to coarse grain size with a densely packed texture) that differ from that of sedimentary carbonates studied worldwide and typically associated with the so-called ACR (argillaceous dolomitic limestones with dolomite rhombs scattered in the fine-grained matrix). Therefore, the presence and distribution of the dedolomitization process appears not to be related to the texture of the aggregates (or the clay content) but to the amount of dolomite in the rock.
- In summary, although dolomitic and calc-dolomitic marbles can develop dedolomitization, they can be used as aggregates for concrete because there is no evidence of deterioration associated with this process (provided they are physically and mechanically suitable for their specific use). However, care must be taken in those samples where strained quartz or another kind of reactive phase can act as silica source for ASR.

Acknowledgments

The authors are deeply indebted to Eng. Oscar Batic for his valuable contribution in the physical tests and Dr. Fernando Colombo for his contribution in the PANalytical X'Pert PRO diffractometer. They also thank CICTERRA (CONICET-UNC), LEMIT-CIC, the Geology Department of UNS-INGEOSUR and CIC from the province of Buenos Aires for their support. Finally, we are grateful to anonymous reviewers for their comments that have improved the manuscript.

References

[1] Swenson EG. A reactive aggregate undetected by ASTM test. ASTM Bull 1957;226:48–51.
[2] Hadley DW. Alkali reactivity of carbonate rocks-expansion and dedolomitization. In: Proceedings of the fortieth annual meeting of the highway research board. vol. 40. Washington, DC: Highw Res Board Proc; 1961. p. 462–74.
[3] Hadley DW. Alkali reactivity of dolomitic carbonate rocks. In: Proceedings, symposium on alkali-carbonate rock reactions. Washington, DC: Highway Res Board, Record 45; 1964. p. 1–20.
[4] Newlon HH, Sherwood WC. An occurrence of alkali-reactive carbonate rock in Virginia. Highway Res Board Bull 1962;355:27–44.
[5] Welp TL, De Young CE. Variations in performance of concrete with carbonate aggregates in Iowa. In: Proceedings, symposium on alkali-carbonate rock reactions. Washington, DC: Highway Res Board, Record 45; 1964. p. 159–77.
[6] Deng M, Han SF, Lu YN, Lan XH, Hu YL, Tang MS. Deterioration of concrete structures due to alkali-dolomite reaction in China. Cem Concr Res 1993;23(5):1040–6.
[7] Tong L, Deng M, Lan X, Tang M. A case study of two airport runways affected by alkali-carbonate reaction. Part one: evidence of deterioration and evaluation of aggregates. Cem Concr Res 1997;27(3):321–8.
[8] Sommer H, Steigenberger J, Zückert U. Vermeiden von Schäden durch Alkalizuschlagreaktion. Schriftenreihe Straßenforschung Heft 2001;504:76.
[9] Katayama T. How to identify carbonate rock reactions in concrete. Mater Charact 2004;53(2–4):85–104.
[10] Katayama T. The so-called alkali-carbonate reaction (ACR) – its mineralogical and geochemical details, with special reference to ASR. Cem Concr Res 2010;40(4):643–75.
[11] Katayama T. Modern petrography of carbonate aggregates in concrete – diagnosis of so-called alkali-carbonate reaction and alkali-silica reaction. In: Fournier B, editor. Marc-André Bérubé symposium on alkali-aggregate reactivity in concrete, 8th CANMET/ACI international conference on recent advances in concrete technology. Montreal, Canada; 2006 (Suppl.). p. 423–44 (not included in the proceedings).

[12] Katayama T. So-called alkali-carbonate reaction – petrographic details of field concretes in Ontario. In: Mauko A, Kosec T, Kopar T, Gartner N, editors. Proceedings of the 13th euroseminar on microscopy applied to building materials. Ljubljana, Slovenia; 2011. p. 15.
[13] Grattan-Bellew PE, Margeson J, Mitchell LD, Min D. Is ACR just another variant of ASR? Comparison of acid insoluble residues of alkali-carbonate reactive limestones and its significance for the ASR/ACR debate. In: Broekmans MATM, Wigum BJ, editors. Proceedings of the 13th international conference on alkali-aggregate reaction in concrete. Trondheim, Norway; 2008. p. 706–16.
[14] Grattan-Bellew PE, Mitchell LD, Margeson J, Min D. Is alkali-carbonate reaction just a variant of alkali-silica reaction ACR = ASR? Cem Concr Res 2010;40(4):556–62.
[15] Katayama T, Sommer H. 2008. Further investigation of the mechanisms of so-called alkali-carbonate reaction based on modern petrographic techniques. In: Broekmans MATM, Wigum BJ, editors. Proceedings of the 13th international conference on alkali-aggregate reaction in concrete. Trondheim, Norway; 2008. p. 850–60.
[16] Katayama T, Grattan-Bellew PE. Petrography of the Kingston experimental sidewalk at age 22 years – ASR as the cause of deleteriously expansive, so-called alkali-carbonate reaction. In: Drimalas T, Ideker JH, Fournier B, editors. Proceedings of the 14th international conference on alkali-aggregate reaction in concrete. Austin, Texas, USA; 2012. p. 10.
[17] Jensen V. The controversy of alkali carbonate reaction: state of art on the reaction mechanisms and behaviour in concrete. In: Drimalas T, Ideker JH, Fournier B, editors. Proceedings of the 14th international conference on alkali-aggregate reaction in concrete. Austin, Texas, USA; 2012. p. 10.
[18] Prinčič T, Štukovnik P, Pejovnik S, De Schutter G, Bosiljkov VB. Observations on dedolomitization of carbonate concrete aggregates, implications for ACR and expansion. Cem Concr Res 2013;54:151–60.
[19] Štukovnik P, Prinčič T, Pejovnik RS, Bosiljkov VB. Alkali-carbonate reaction in concrete and its implications for a high rate of long-term compressive strength increase. Constr Build Mater 2014;50:699–709. <http://dx.doi.org/10.1016/j.conbuildmat.2013.10.007>.
[20] Batic OR, Cortelezzi C, Maiza PJ, Marfil SA, Milanesi CA, Pavlicevic R. Reacción deletérea de algunas rocas dolomíticas en hormigones. In: Asociación Argentina de Tecnología del Hormigón, editor. Proceedings of the 10th technical meeting Ing. Juan F. vol. 2. García Balado, Olavarría, Buenos Aires, Argentina; 1991. p. 95–113.
[21] Batic OR, Milanesi CA. Experiencias sobre la reacción álcali-carbonato con rocas dolomíticas. Revista Hormigón 1991;19:15–29.
[22] Milanesi CA, Batic OR. Alkali reactivity of dolomitic rocks from Argentina. Cem Concr Res 1994;24(6):1073–84.
[23] Milanesi CA, Marfil SA, Batic OR, Maiza PJ. The alkali-carbonate reaction and its reaction products – an experience with Argentinean dolomite rocks. Cem Concr Res 1996;26(10):1579–91.
[24] Milanesi CA, Marfil S, Maiza PJ, Batic OR. An expansive dolostone from Argentina – the common dilemma: ACR or another variant of ASR?. In: Drimalas T, Ideker JH, Fournier B, editors. Proceedings of the 14th international conference on alkali-aggregate reaction in concrete. Austin, Texas, USA; 2012. p. 8.
[25] Locati F, Marfil SA, Maiza PJ, Baldo E. Characterization of ASR products in a 40-year-old highway. Province of Córdoba, Argentina. In: Drimalas T, Ideker JH, Fournier B, editors. Proceedings of the 14th international conference on alkali-aggregate reaction in concrete, Austin, Texas, USA; 2012. p. 8.
[26] Ozol MA. Alkali-carbonate rock reaction. In: Lamond JF, Pielert JH, editors. Significance of test and properties of concrete & concrete-making materials. United States: ASTM International; 2006. p. 410–24. ASTM STP 169D, [Chapter 35].
[27] Locati F, Falcone D, Batic O, Marfil S. Evaluación del potencial comportamiento reactivo de mármoles de la provincia de Córdoba frente a la reacción álcali-carbonato. In: Sota JD, Ortega NF, Moro JM, editors. V Congreso Internacional – 19 Reunión Técnica "Ing. Oscar R. Batic". Bahía Blanca, Buenos Aires, Argentina; 2012. p. 127–34.
[28] ASTM C1293-08b. Standard test method for determination of length change of concrete due to alkali-silica reaction. Annual Book of ASTM Standards, American Society for Testing and Materials; 2008.
[29] ASTM C586–11. Standard test method for potential alkali reactivity of carbonate rocks as concrete aggregates (Rock-Cylinder Method). Annual Book of ASTM Standards, American Society for Testing and Materials; 2011.
[30] CSA A23.2-26A. Determination of potential alkali-carbonate reactivity of quarried carbonate rocks by chemical composition. Canadian Standards Association. Ontario, Canada; 2004.
[31] Lu D, Fournier B, Grattan-Bellew PE, Xu Z, Tang M. Development of a universal accelerated test for alkali-silica and alkali-carbonate reactivity of concrete aggregates. Mater Struct 2008;41(2):235–46.
[32] Xu Z, Shen Y, Lu D. Main parameters in the new test method for alkali-silica reactivity. J Nanjing Univ Chem Technol (in Chinese) 1998;20(2):1–7.
[33] IRAM 50000. Cemento. Cemento para uso general. Composición, características, evaluación de la conformidad y condiciones de recepción. IRAM, instituto Argentino de normalización y certificación. Buenos Aires, Argentina; 2010.
[34] ASTM C150/C150M-12. Standard specification for portland cement. Annual Book of ASTM Standards, American Society for Testing and Materials; 2012.
[35] IRAM 1501–2. Tamices de ensayo. Tela de tejido metálico, chapa metálica perforada y lámina electroformada. Tamaños nominales de abertura. IRAM, instituto Argentino de normalización y certificación. Buenos Aires, Argentina; 2002.
[36] Whitney DL, Evans BW. Abbreviations for names of rock-forming minerals. Am Mineral 2010;95(1):185–7.
[37] ASTM D3042–09. Standard test method for insoluble residue in carbonate aggregates. Annual Book of ASTM Standards, American Society for Testing and Materials; 2009.
[38] Hutchison CH. Laboratory handbook of petrographic techniques. New York: John Wiley & Sons Inc.; 1974.
[39] Rasband WS. ImageJ. U. S. National Institutes of Health, Bethesda, Maryland, USA. <http://imagej.nih.gov/ij/; 1997-2012>.
[40] Chung FH. Quantitative interpretation of x-ray diffraction patterns of mixtures. I. Matrix-flushing method for quantitative multicomponent analysis. J Appl Crystallogr 1974;7(6):519–25.
[41] Vernon RH. A practical guide to rock microstructure. United Kingdom: Cambridge University Press; 2004.
[42] Wigum BJ. Examination of microstructural features of Norwegian cataclastic rocks and their use for predicting alkali-reactivity in concrete. Eng Geol 1995;40(3–4):195–214.
[43] Leemann A, Holzer L. Alkali-aggregate reaction – identifying reactive silicates in complex aggregates by ESEM observation of dissolution features. Cem Concr Compos 2005;27(7–8):796–801.
[44] Grattan-Bellew PE, Beaudoin JJ. Effect of phlogopite mica on alkali-aggregate expansion in concrete. Cem Concr Res 1980;10(6):789–97.
[45] Lagerblad B. Alkali release from silicate minerals and alkali-silica reaction in concrete. In: Drimalas T, Ideker JH, Fournier B, editors. Proceedings of the 14th international conference on alkali-aggregate reaction in concrete. Austin, Texas, USA; 2012. p. 6.
[46] Katayama T, Oshiro T, Sarai Y, Zaha K, Yamato T. Late-expansive ASR due to imported sand and local aggregates in Okinawa Island, southwestern Japan. In: Broekmans MATM, Wigum BJ, editors. Proceedings of the 13th international conference on alkali-aggregate reaction in concrete, Trondheim, Norway; 2013. p. 862-73.
[47] Xiaoming S, Min D, Lingling X, Daqing K, Mingshu T. Reaction products in systems of $CaMg(CO_3)_2$. In: Drimalas T, Ideker JH, Fournier B, editors. Proceedings of the 14th international conference on alkali-aggregate reaction in concrete. Austin, Texas, USA; 2012. p. 10.
[48] Batic OR, Milanesi CA, Sota JD. Effects of alkali-silica and alkali-carbonate rock reaction on aggregate-mortar bond. In: Berube MA, Fournier B, Durand B, editors. Proceedings of the 11th international conference on alkali-aggregate reaction in concrete. Quebec, Canada; 2000. p. 1–10.
[49] Katayama T. Rim-forming dolomitic aggregate in concrete structures in Saudi Arabia – Is dedolomitization equal to the so-called alkali-carbonate reaction?. In: Drimalas T, Ideker JH, Fournier B, editors. Proceedings of the 14th international conference on alkali-aggregate reaction in concrete. Austin, Texas, USA; 2012. p. 10.